27th SINGAPORE YOUTH SCIENCE FESTIVAL
SECONDARY & PRE-UNIVERSITY SCIENCE FAIR 2004

Level: **Pre-University**

Category: **ENVIRONMENT**

Project Title: **The Investigation of the Effects of Solar Flares on Decametric Frequencies**

Team Members:

Tey Zhi Hao Joseph (Team Leader)
Toh Weide
Li Chi Sheng
Ng Wei Tat Leonard
Suen Yeu Arng
Angie Theonis Teoh

Sponsor Teacher(s):

Mr Tan Hoe Teck

School: **Catholic Junior College**

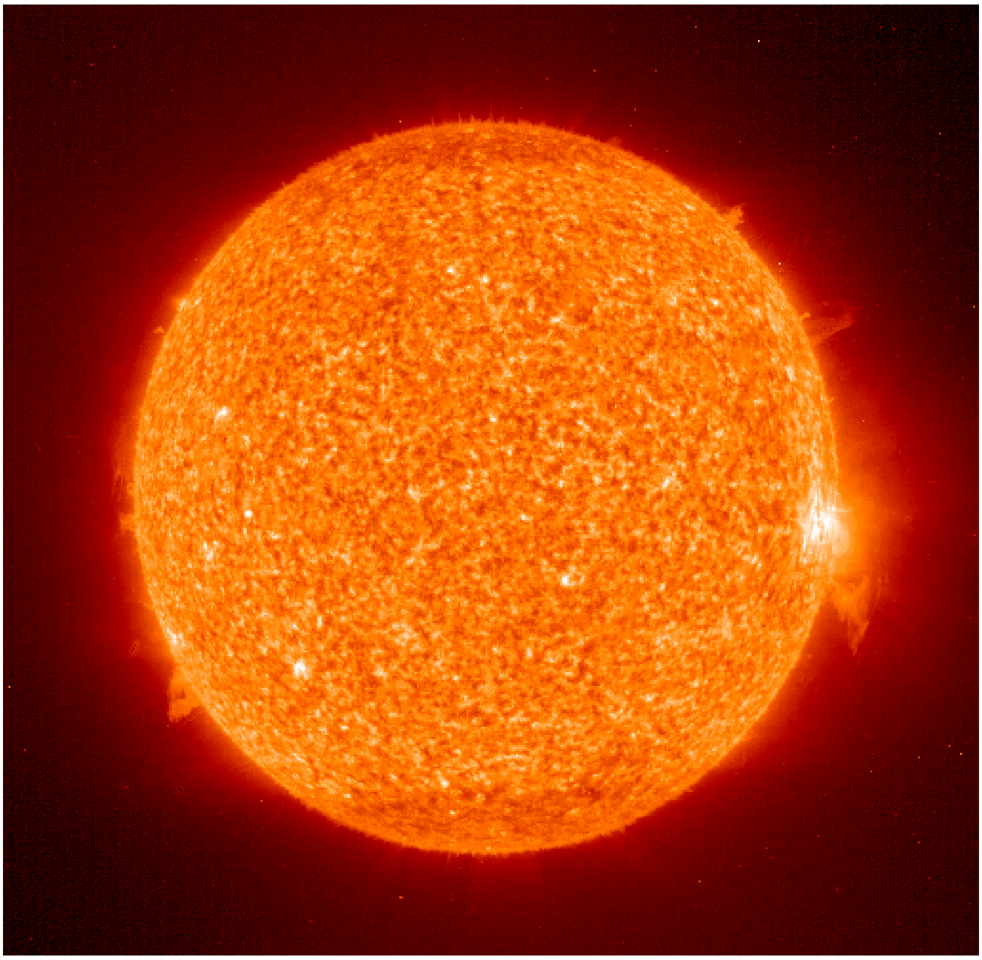

The Investigation of the Effects of Solar Flares on Decametric Frequencies

Done By: Tey Zhi Hao Joseph (Team Leader)
Toh Weide
Li Chi Sheng
Ng Wei Tat Leonard
Suen Yeu Arng
Angie Theonis Teoh

Catholic Junior College

Contents

Acknowledgements

Very special and big thanks to Mr. Richard S. Flagg, radio astronomer at the University of Hawaii Windward Community College Radio Observatory (WCCRO), for his guidance through his various e-mails as well his passion in sharing his lifelong profession with us. Thanks also to Mr. Sasi Nayar (9V1SM/VU3SNM), Treasurer of Singapore Amateur Radio Transmission Society (SARTS), for sharing his hobby of amateur radio, and to Brother Paul Rogers, Principal of Catholic Junior College, for providing the necessary funds needed to set up our "DIY" amateur radio observatory in college. Last but not least, a very big thank you to our teacher in charge, Mr. Tan Hoe Teck, for introducing us the possibility of conducting amateur radio astronomy research in Singapore and for sticking through with us since day one.

1. Abstract

Our project was conducted over a span of 5 months (from November 2003 till end March 2004) with the main purpose of detecting radio signals due to solar flares using an amateur radio station, and to draw conclusions on how these signals affect frequencies in the decametric range of 3MHz – 40MHz. This range is also known as the HF (high frequency) communication band and is widely used by governmental and commercial agencies as well as private users for long distance radio communication.

In our main findings, we found that as the degree of X-ray radiation produced by a solar flare increased, the greater was the intensity of radio interference from the sun. It was also discovered that solar flares of increasing magnitudes caused radio blackouts, i.e. complete absorption of signals due to X-ray ionization in the ionosphere, at lower frequencies of the decametric range. From this we concluded that the greater the level of X-ray energy, the deeper the penetration into the atmosphere and hence the ionization of lower altitudes to cause signal absorption at lower decametric frequencies.

2. Declaration of Degree of Guidance

The guidance received during the course of our project was through e-mail correspondence with Mr. Richard Flagg where our questions or doubts would be clarified by him. He also provided us with the computer software and radio receiver needed to carry out our data recordings. All recorded data was collected independently by either using our station or recorded remotely on a computer when connected to a foreign radio observatory via the internet. As our guidance was through e-mail tele-mentoring, Mr. Flagg's lack of physical presence meant that majority of the groundwork and research had to be done by us, such as the construction of our amateur radio station in college. Our teacher, Mr Tan, as well as Mr Nayar from SARTS, only provided us with books and research materials that we requested for during our course of study.

3. Introduction

The sun's presence in our solar system is the reason why life on Earth exists. However, it is also a force to reckon with. Each day, the sun bathes us with electro-magnetic energy of all forms that could well destroy life if not for the atmosphere's protection which shields us from the solar radiation. Although we are safe from such radiation, the sun's effect on our atmosphere plays a major role in affecting radio communications. In this modern world of ours, radio communications forms the backbone of daily activities for many industries, most notably the marine sector. The band of frequencies in use for radio communications is known as the decametric range of 3 MHz – 40 MHz and is termed the HF (high frequency) band. This project was done out of our own personal interests in radio astronomy as well as amateur radio communication. As the world today relies a lot on communications, it was also our own curiosity which led us to investigate how solar flares can affect such communications.

Our project's main focus is detecting radio emissions due to solar flares in the decametric range and to investigate how these signals are of a cause of concern to radio communications.

4. Theoretical Background

Sunspots and Solar Flares

Sunspots (Figure 4.1) are regions of intense localized magnetic lines caused by the varying rotational speed of the sun. Because the sun is a ball of gas, its equator tends to rotate faster than its poles. Hence, magnetic field lines which normally run independently from pole to pole are dragged together and twisted. Hot gases pushing these flux lines break through to the sun's surface and the distorted field lines slows down rising convection currents, causing the region to cool. These cooler areas appear as dark spots with respect to its hotter surroundings (Jay M. Pasachoff, 1979). A flare (4.2) is defined as a sudden explosion on the sun's surface (John D. Kraus, 1986). They occur near sunspots, usually along the dividing line between areas of oppositely directed magnetic fields, where magnetic energy built up in the solar atmosphere is suddenly released (Richard Flagg, 2000). During which, radiation is emitted across the entire electromagnetic spectrum.

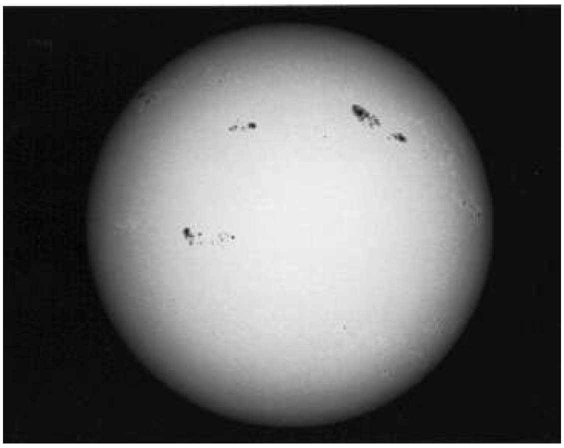

Figure 4.1 *(Source: archive.ncsa.uiuc.edu)*

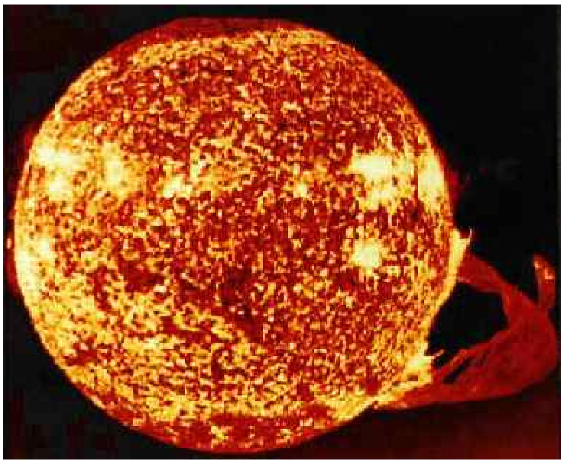

Figure 4.2 *(Source: archive.ncsa.uiuc.edu)*

The Ionosphere

At an altitude of 48 km to 400 km, intense solar radiation during the day causes the atoms in the atmospheric gases to break-up into ions, thus forming a sphere of ionised gas. There are four distinct layers in the ionosphere designated the D, E, F_1 and F_2 layers (Figure 4.3). The ionic condition of this area of the atmosphere causes radio waves to bounce back to earth and is termed as sky-wave propagations. D and E layers cause decametric frequencies between 3 MHz to 25 MHz to be reflected whilst higher frequencies between 26MHz to 40MHz are reflected by the F layers (Forest Barker, 1987) as seen in Figure 4.4. Frequencies above 40MHz will simply penetrate the ionosphere and into space. As ionisaton occurs only when sunlight is present, the ionosphere slowly disappears (de-ionize) in the night, allowing all radio frequencies to pass through. It reappears again in the morning when sunlight returns.

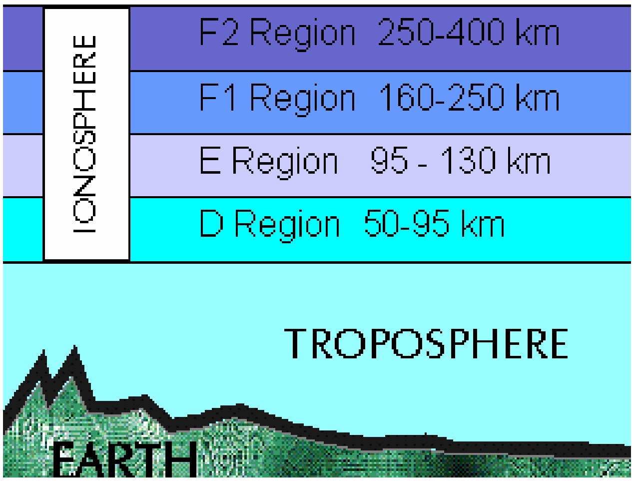

Figure 4.3 *(source: library.thinkquest.org)*

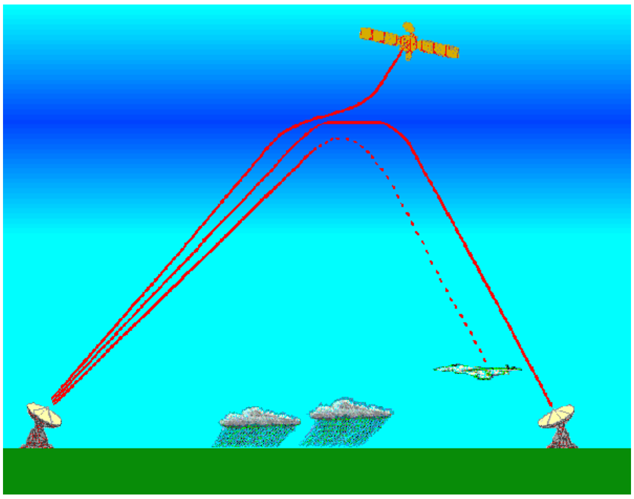

Figure 4.4 *(Source: www.arsc.edu/science/ionosphere.html)*

Radio Noise Bursts and Radio Blackouts

Radio noise burst are often associated with flares and are observed in the 4 to 400 MHz frequency range. Even though the daytime ionosphere can reflect much of the energy of solar bursts back into space, most bursts are still strong enough to penetrate and be detected by a HF receiver. There are five classifications of radio noise bursts but only two are associated with a flash phase solar flare: Type III and V (John D. Kraus, 1986). **Type III** bursts drift rapidly from high to low frequencies at about 20 MHz per second and occur at the same time as the flash phase of the solar flare while **Type V** events cover a large band of frequencies (broadband). Radio blackouts are known to precede radio noise bursts resulting in the complete attenuation of radio signals due to absorption. This is caused by increased ionization in the ionosphere due to X-rays (Wayne Tomasi, 1988).

Project Aims

From our findings, we aim to answer two key questions: the type of solar radio emissions affecting decametric frequencies and the nature of radio blackouts caused by a solar flare.

5. Resources and Apparatus

The internet was the main information resource utilised in the project. It provided us with the theoretical background as well as the technical knowledge needed to interpret our data. It also provided us the ability to verify our data and to classify solar flares through the access of Geostationary Operational Environmental Satellite (GOES) as well as SOHO (The Solar and Heliospheric Observatory) scientific data.

Figure 5.1
(Source: CJC Astro-Club)

The main resource used for data collection is our apparatus, an antenna system connected to a radio receiver and a computer strip-chart recorder as seen in Figure 5.1. **The radio receiver** used was a tuner which tunes over a narrow range of frequencies (+/- 150 KHz) centred on 20.1 MHz. Since the HF ranges from 3 MHz to 40MHz, 20.1MHz was chosen as it is the centre of this range. **The antenna** design selected is called the duel dipole system (Figure 5.2) and is preferred over a single dipole due to its greater sensitivity. A dipole antenna works by suspending a wire of

Figure 5.2 *(Source: CJC Astro-Club)*

length equivalent to approximately half a wavelength of the resonant frequency. The formula for determining the length L of a dipole antenna in metres is: L= 142/f

At the centre of the antenna lies the antenna feed-point which connects the antenna wire to a coaxial transmission line (Figure 5.3). When an antenna

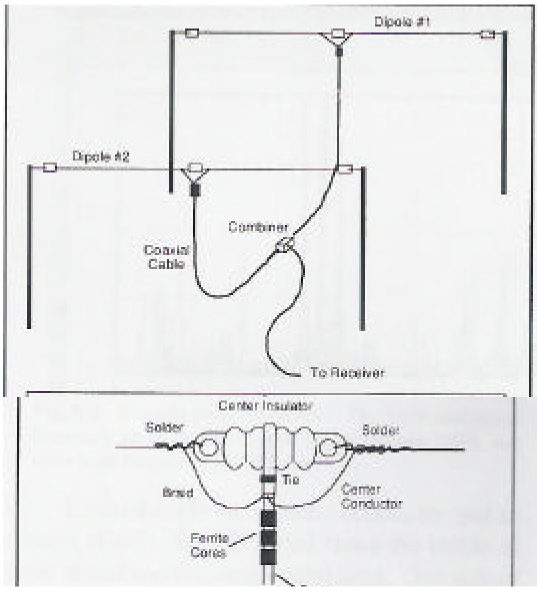

Figure 5.3 *(Source: Listening to Jupiter)*

intercepts electromagnetic waves from a distant transmitter, a radio frequency (RF) voltage is developed across the antenna terminals in the form of a standing wave (Figure 5.4). The antenna is suspended ¼ wavelengths above the ground so as to allow the other half of the wave to be reflected. The RF voltage is then transmitted through the coaxial cable via the feed-point into the receiver. By using two dipoles, we also are able to vary the antenna beam patterns by changing the position of the feed-points. When the two are opposite, the antennas are said to be anti-phase; when in the same direction, it is in-phase (Figure 5.5). This changes the beam pattern which is illustrated in figure 5.6.

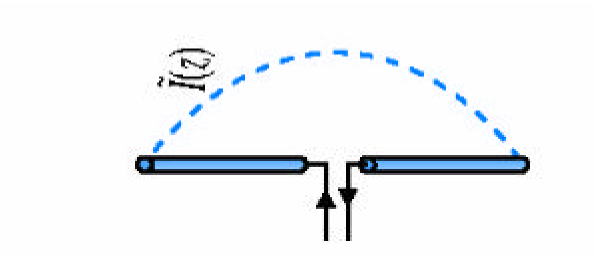

Figure 5.4 *(Source: www.arrl.org)*

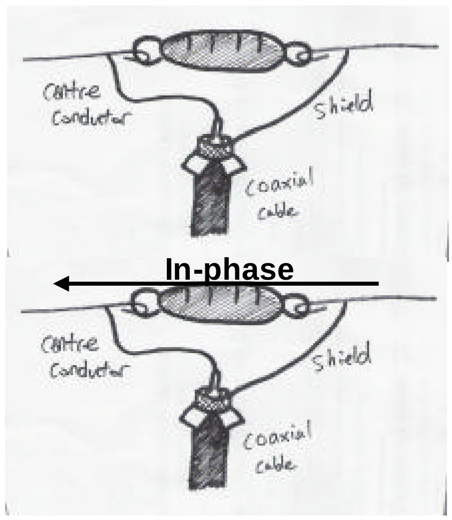

Figure 5.5
(Source: Listening to Jupiter)

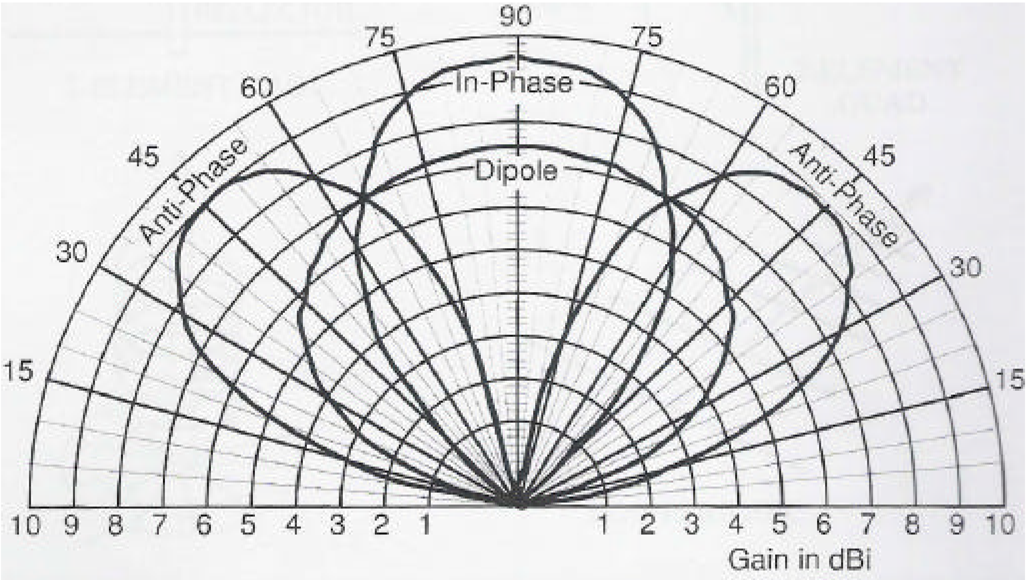

Figure 5.6 *(Source: Listening to Jupiter)*

By changing the angle of the beam-widths, we are thus able to “aim” the antenna according to the sun’s position in the sky.

6. Methodology and Procedures

Solar emissions were recorded using either two methods: a computer strip chart connected to our antenna system or remotely to a foreign radio observatory, or a computer spectrogram connected remotely to a radio observatory in the US. The computer strip chart plots an intensity readout relative to the background noise radiation (Y-axis) against time (X-axis) while the spectrograms record signals received over a band of frequencies (Y-axis) by scanning through them simultaneously during a certain time duration (X-axis). Both are illustrated in the examples of Figures 6.1 & 6.2 respectively.

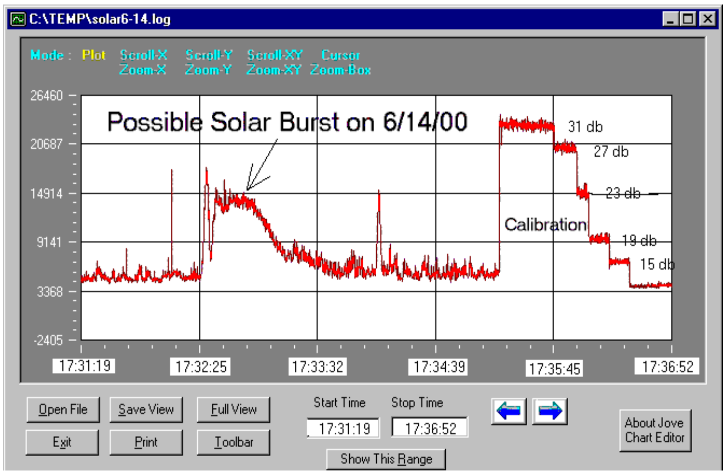

Figure 6.1 *(Source: www.radiosky.com)*

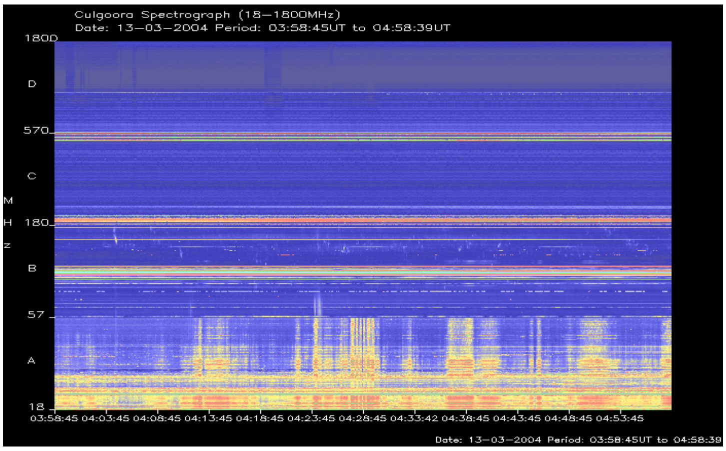

Figure 6.2 *(Source: www.ips.gov.au)*

As the probability of solar emissions are high only when a large sunspot group is present, our data collection dates were thus very subjective to the sun's present activity and are carried out based on forecasts made by a space weather monitoring agency such as the Australian Space Weather Agency's Ionospheric

Prediction Service (IPS). Hence, no definite observation dates were scheduled and all results were obtained on separate and random events. Data could only be received during the day when the sun faces us, and all observations are conducted at noon up to mid afternoon when it is most intense. We relied on both data collected live by our own station during local noon time as well as those collected remotely by our computer data loggers when connected via the internet to a radio observatory on the other side of the world. Data collection via the internet allowed us the capability to carry out observations whilst we are experiencing night by connecting to an American observatory or any other observatory around the world experiencing noon. This meant that at least 18 hours of monitoring could be done continuously. Recent unforeseen monsoon conditions in 2004 prevented us from data recording as the threat of lightning was too much a risk for field observations. Thus, the 2004 data presented in the following sections had to be recorded over the internet. In the past 6 months, only 2 major sunspot groups have appeared that allowed us to conduct successful radio observations. Our data therefore originates from these following months: November 2003 and March 2004.

Our spectrogram or strip-chart readings are first verified and classified before being used for analysis. For this we employ a 3 step approach as seen in Chart 6.1 and illustrated in chart 6.2. As all recordings are done and synchronized using Universal Time (UT), confirmation of data can be done by comparing the secondary data source to see if a similar solar flare occurred at the same time.

Chart 6.1

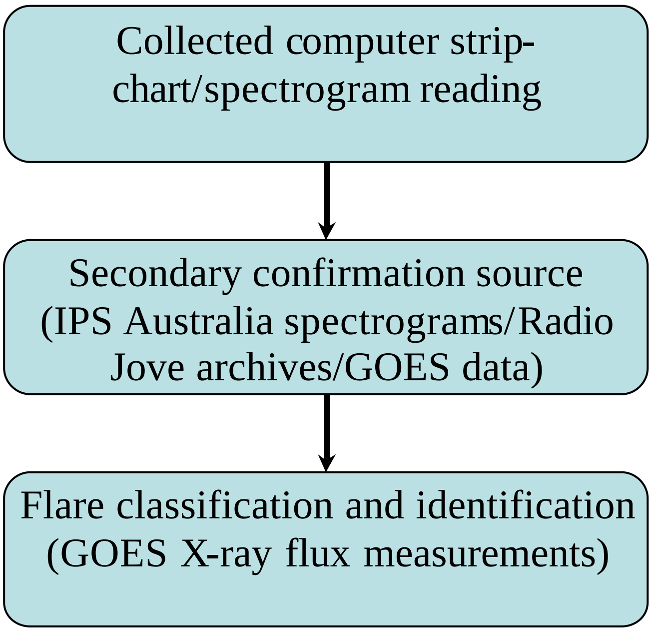

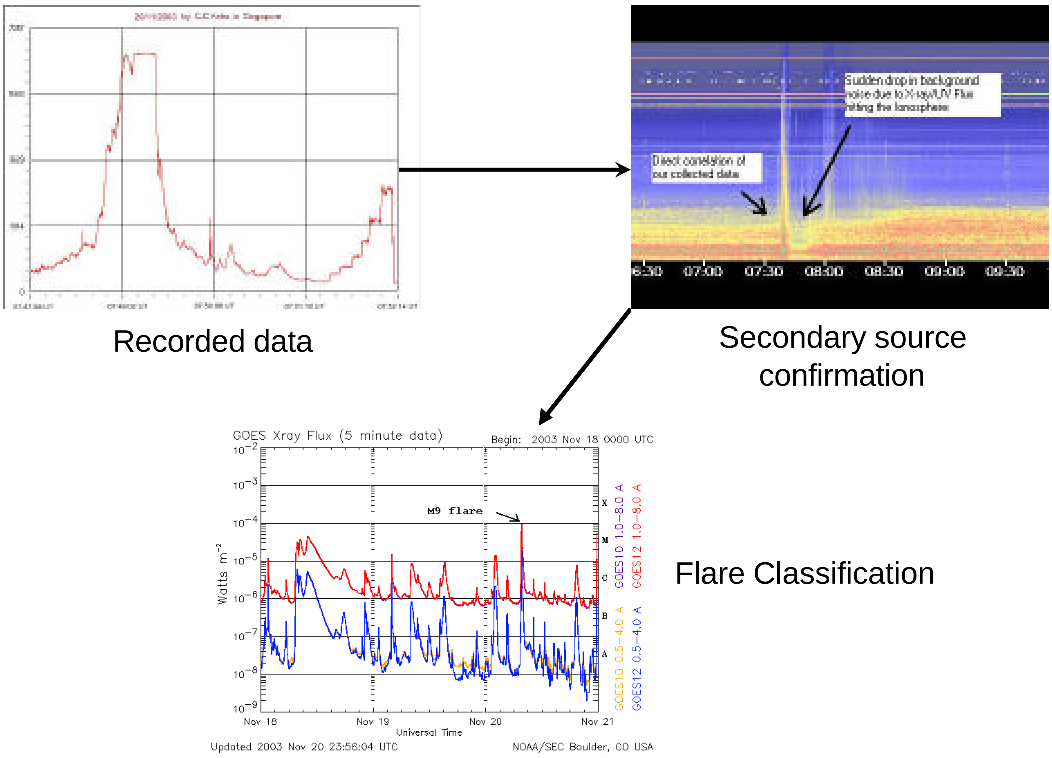

Chart 6.2

Secondary sources come from either of the three: IPS spectrogram images, posted data by other Radio Jove participants on the web archives or X-ray flux data from the National Oceanic and Atmospheric Administration's (NOAA) Geostationary Operational Environmental Satellite (GOES). Our recorded flare is then classified into its specific class by referring to GOES X-ray flux density measurements.

With the identification of recorded flares and the use of strip-charts as well as spectrogram images, a correlation is made between these sources. An observation is then made by interpreting the images to see if it exhibits a radio blackout and to identify the flare's burst characteristics.

7. Data Findings

Altogether, four different flare classifications were recorded and selected: one X, M, C and B class flare from the two separate months of November 2003 and March 2004, with the X & M class and C & B class flares originating from each respective month. Each set of data includes a strip-chart recording and/or spectrogram, solar images taken by SOHO and an X-ray flux density chart by GOES.

The recordings on the computer strip-charts as well as the spectrogram images serves as the basic mean of detecting and identifying a solar flare and its corresponding burst type. It also serves the purpose as an indicator as to whether a radio-blackout took place. The image of the sun accompanying each observation provides us with an idea of the current solar activity by displaying the sunspots as well as surface activity present at the time of observation. Lastly, the GOES X-ray flux measurement chart gives us an indication of the flare's classification as well as the approximate magnitude of the intensity of X-ray radiation. All strip-chart as well as spectrogram recordings were recorded within the decametric frequency range of 20 MHz and logged using universal time (UT) so as to assists us in a fair comparison of our data. Each of the following data is accompanied by a summary.

The Solar Flare of November 4, 2003

Between 1941UT and 1959UT, the most explosive solar flare in history was recorded for the first time (See Image 7.2 and Figure 7.1). The solar flare was a result of the huge sunspot group 486 (Image 7.1) located on the sun's eastern limb which measured some 15 Earth diameters across. It was identified by GOES as an X28 class flare with a record X-ray flux density of at least $2.8X10^{-3}$ Wm^{-2} (Figure 7.3). The flare was seen to exhibit a type III burst characteristic. As the flare occurred at 0400hrs local time, we were unable to record the signal. However, we managed to receive the data from a foreign observer located in Minnesota, USA. A sudden drop in the background noise radiation levels was observed immediately after the flare (Figure 7.2).

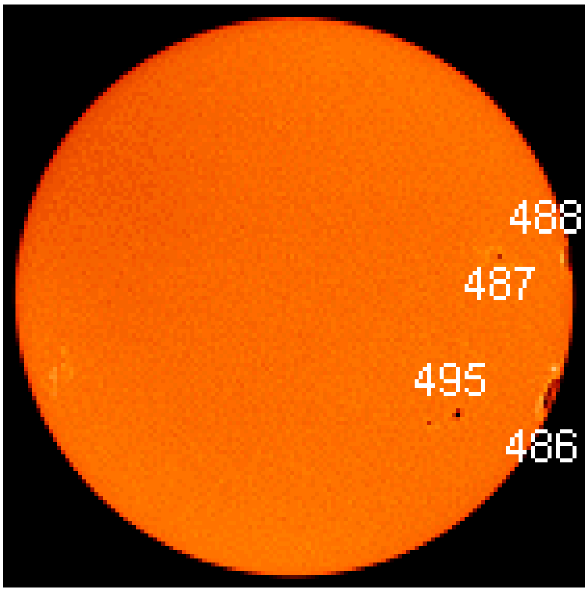

Image 1

(Source: www.spaceweather.com/archive.php)

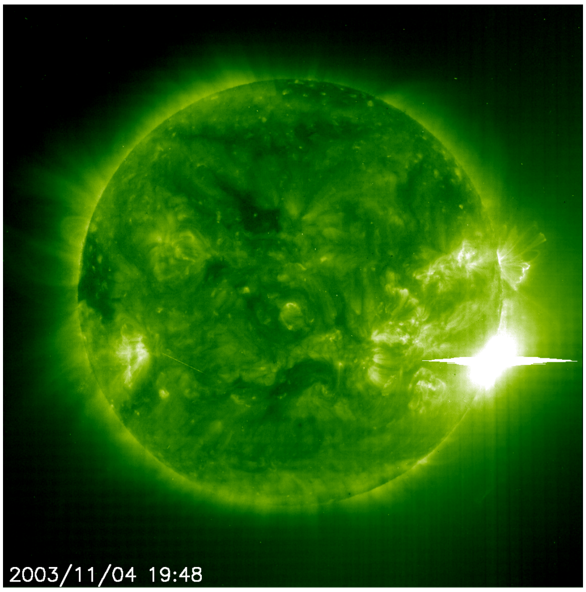

Image 2

(Source: http://sohowww.nascom.nasa.gov/)

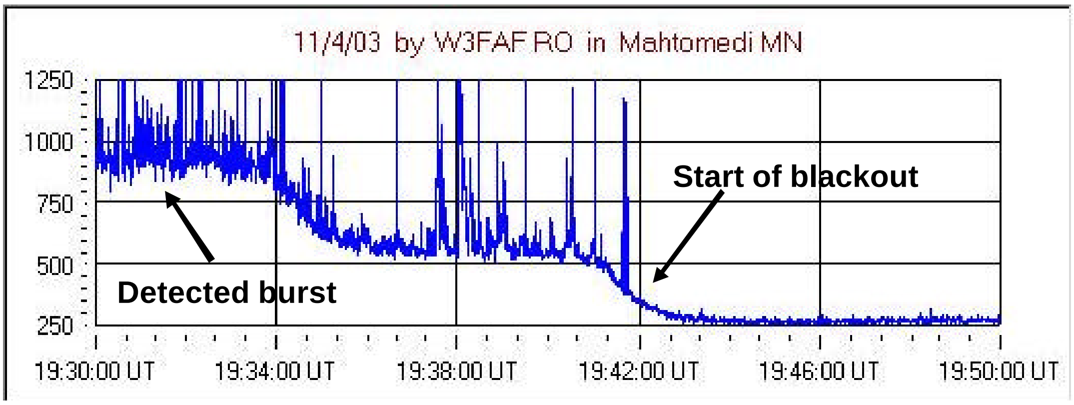

Figure 7.1

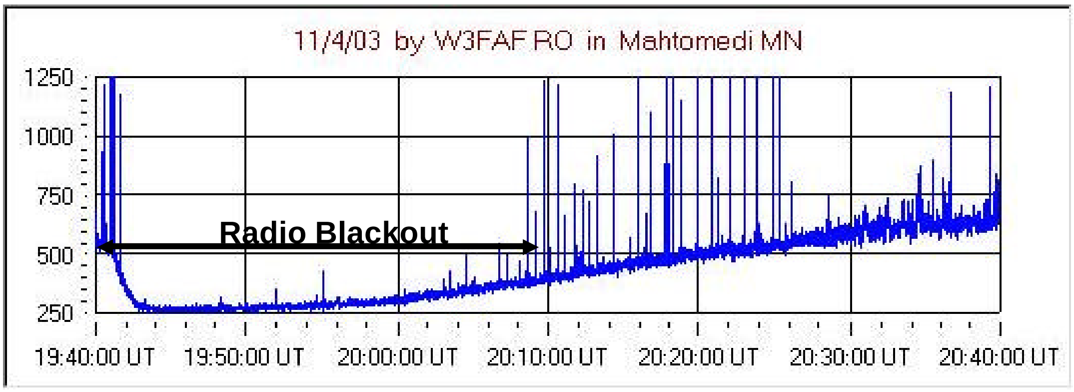

Figure 7.2

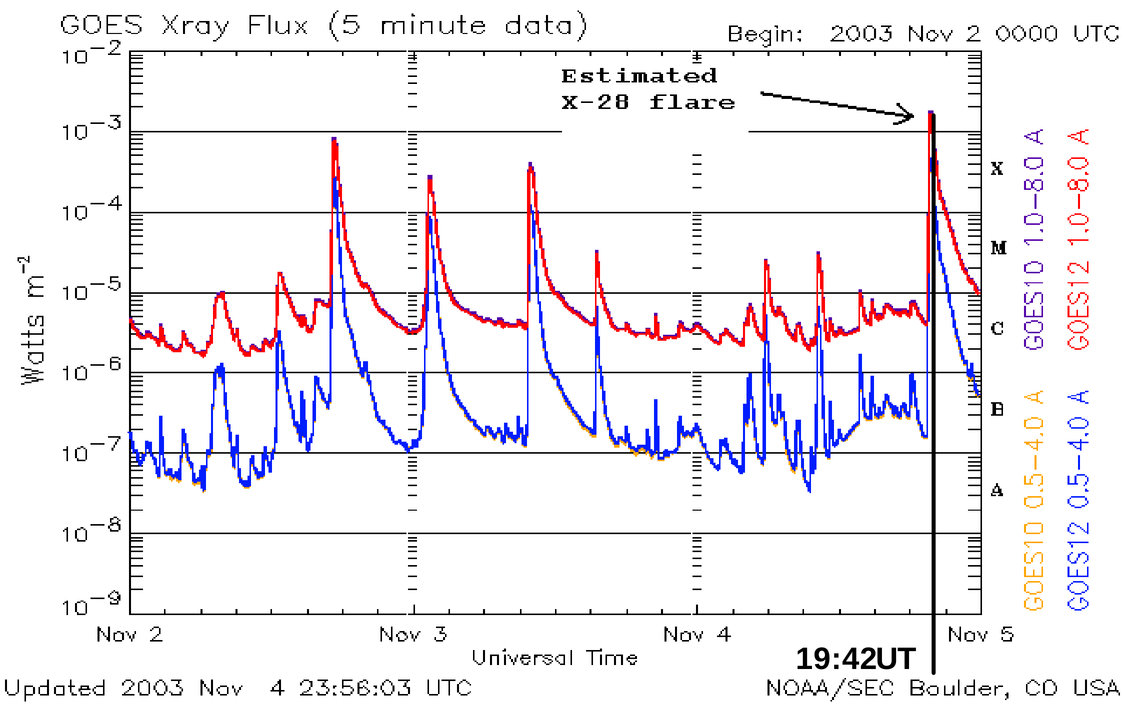

Figure 7.3

(Source: www.spaceweather.com/archive.php)

The Solar Flare of November 16, 2003

16 days after the November 4th solar flare was observed another similar X-ray flare was recorded on November 20th by our own station. This flare came from the exact same sunspot group 486 (Image 7.3 and 7.4) but 16 days later on the sun's western limb after the sun experienced half a rotation. Between 0747UT and 0750UT, a similar type III solar burst was recorded and the intensity of the flare was so great that it caused our receiver to saturate, resulting in the flat peak as seen in Figure 7.4. It was confirmed by GOES as an M9 class flare with an X-ray flux density of $9.0X10^{-5}$ Wm^{-2} (Figure 7.5). Another radio blackout was observed, recorded and confirmed by two independent spectrogram records taken from IPS Australia right after the M-class flare struck us (Figures 7.6 & 7.7)

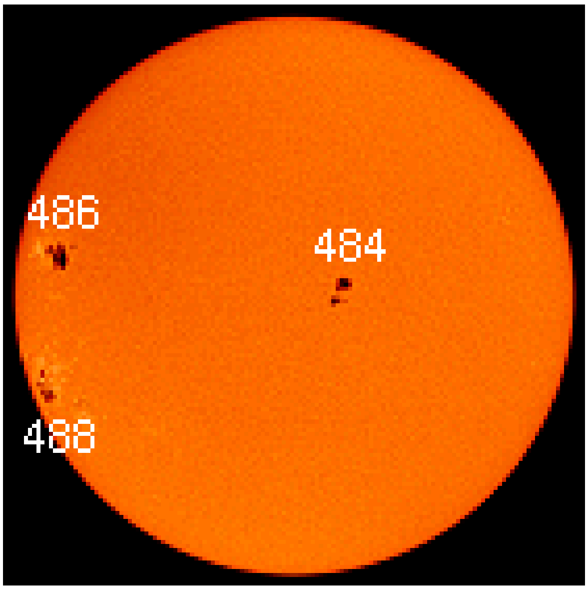

Image 7.3
(Source: www.spaceweather.com/archive.php)

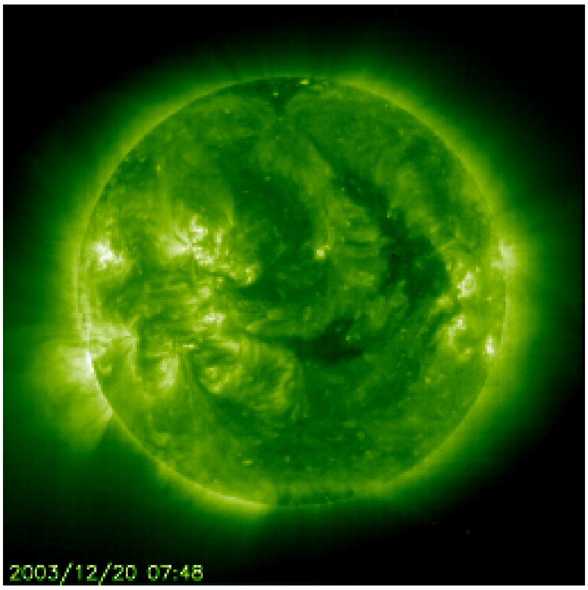

Image 7.4
(Source: http://sohowww.nascom.nasa.gov/)

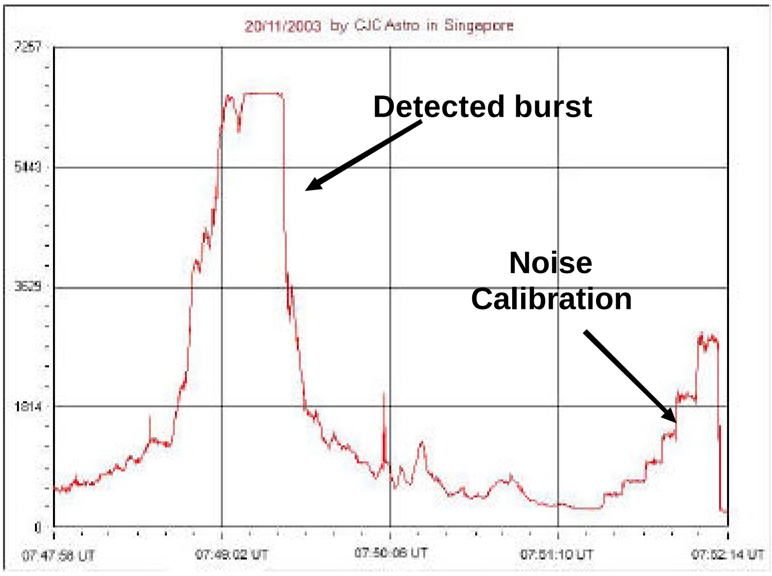

Figure 7.4

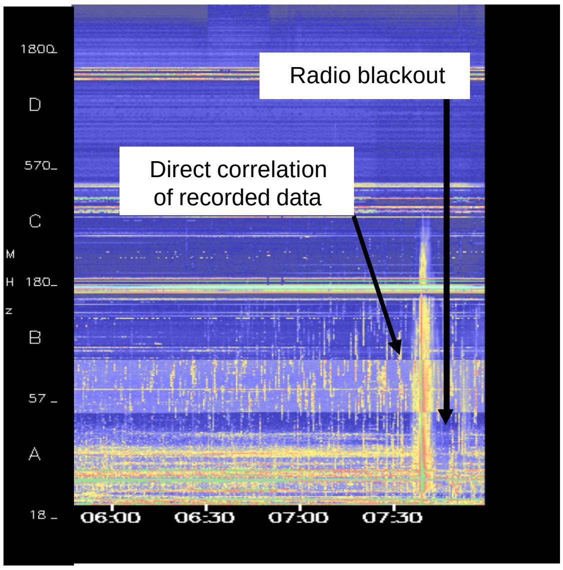

Figure 7.6 *(Source: www.ips.gov.au)*

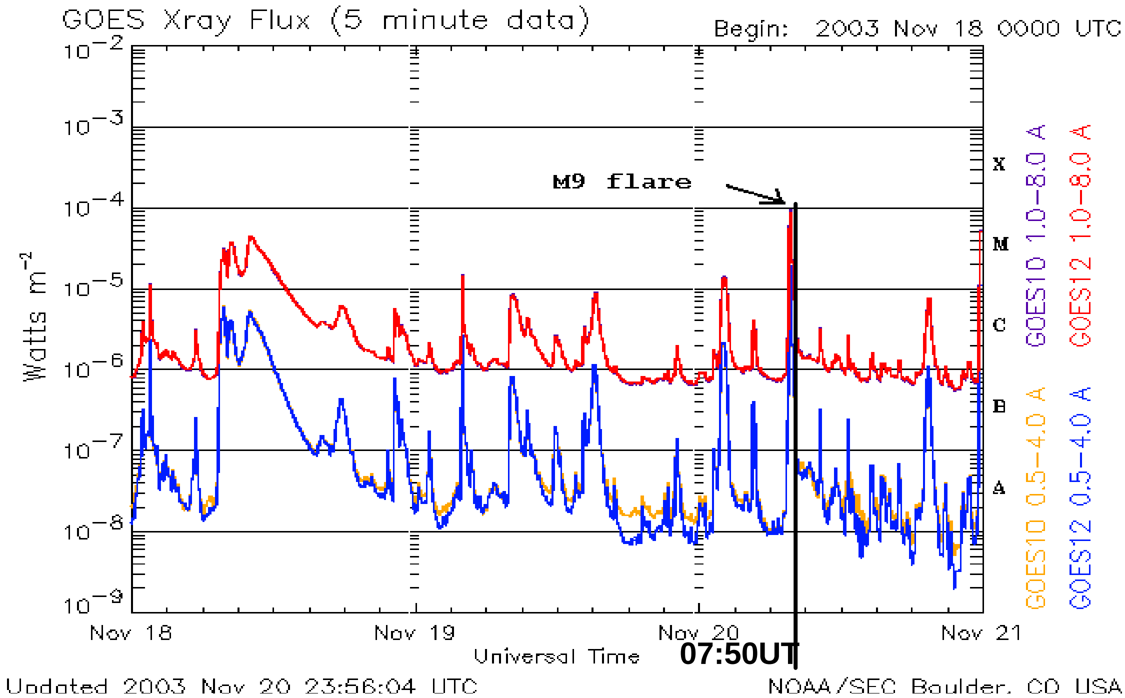

Figure 7.5 *(Source: www.spaceweather.com/archive.php)*

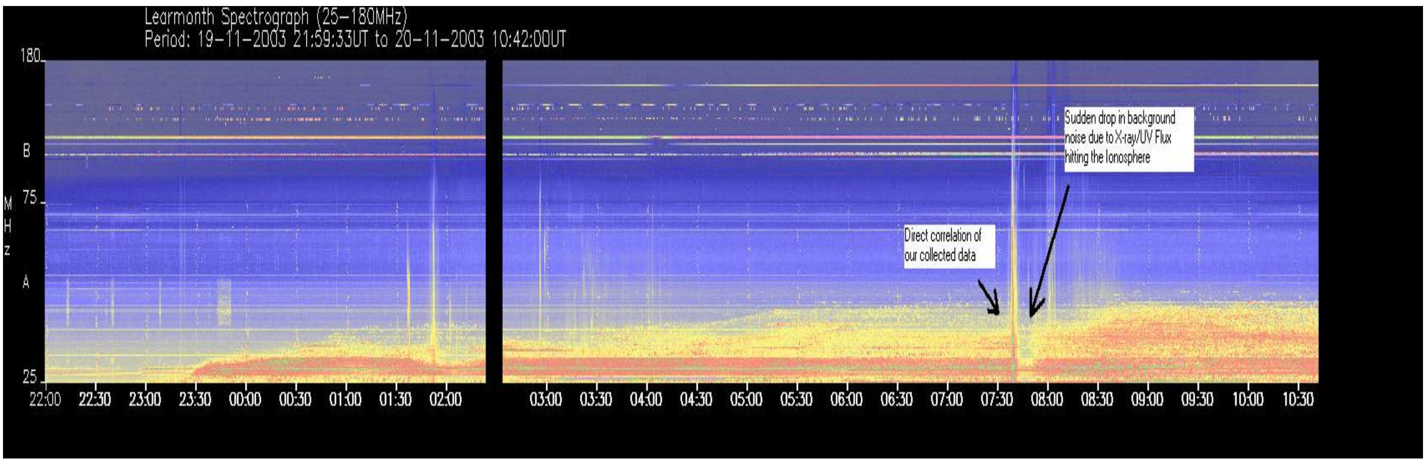

Figure 7.7 *(Source: www.ips.gov.au)*

The Solar Flare of March 10, 2004

During the month of March 2004, the return of another sun spot group, number 570 which measured 10 Earth diameters (Images 7.5 & 7.6), gave us a second opportunity to further study the solar flare effects on the Ionosphere. The first burst recorded remotely using a computer spectrogram on March 10th 2004 at 1850 UT was collected through WCCRO in Hawaii. A secondary observer located in Minnesota, USA, provided us with a strip-chart recording confirming the burst detected at 20 MHz. The flare was identified as a Type III solar burst (Figure 7.8) and classified by GOES as a B7 flare with an X-ray flux density measuring 7.0×10^{-7} Wm^{-2} (Figure 7.10). Although it was recorded as a solar flare, no radio blackout was observed (Figures 7.8 & 7.9).

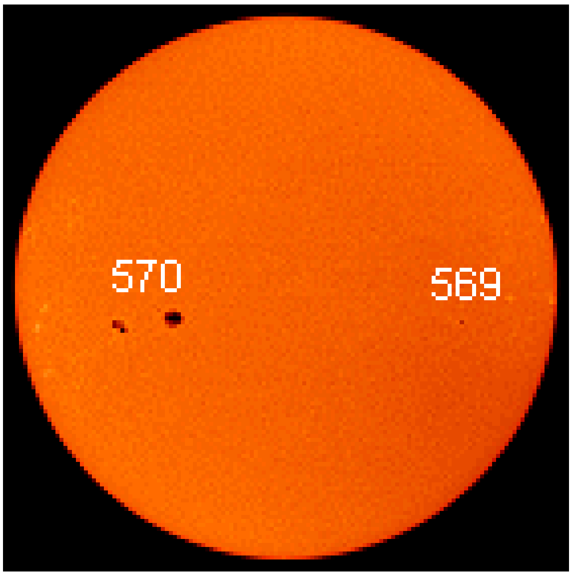

Image 7.5 *(Source: www.spaceweather.com/archive.php)*

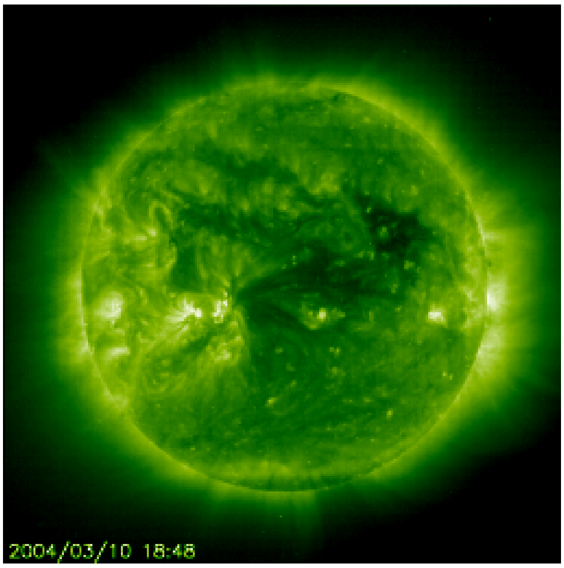

Image 7.6
(Source: http://sohowww.nascom.nasa.gov/)

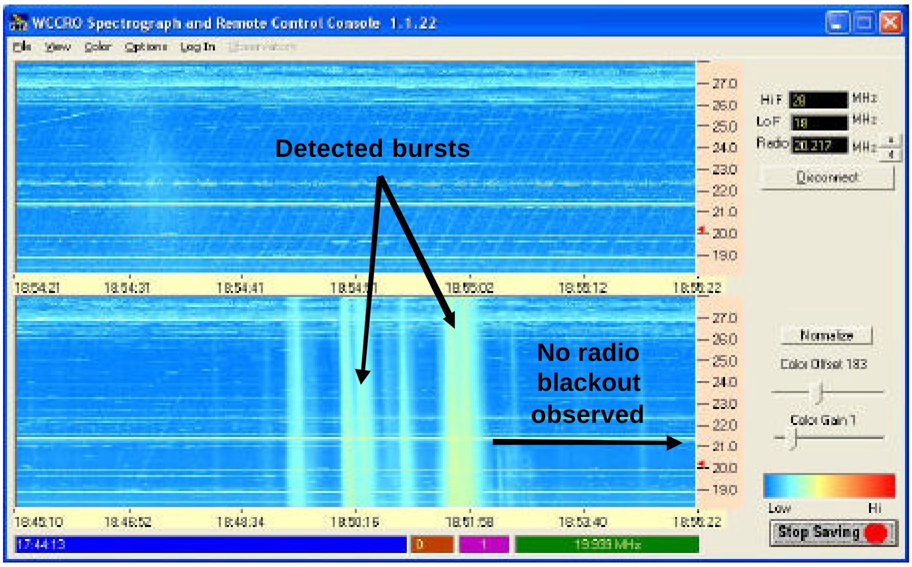

Figure 7.8

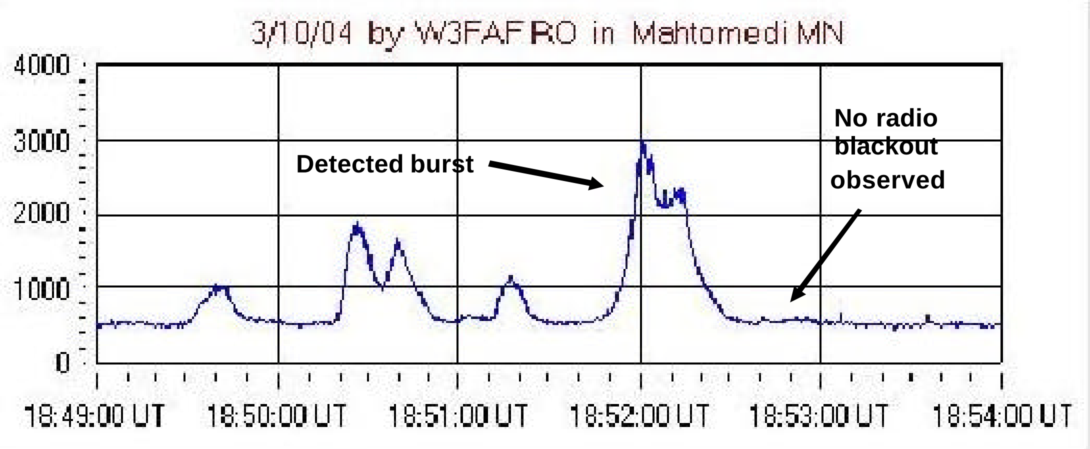

Figure 7.9

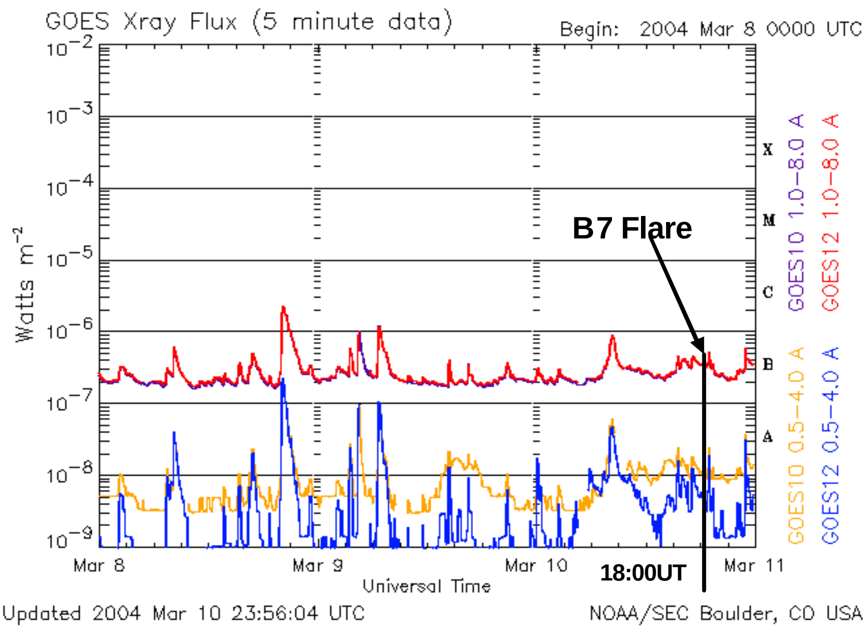

Figure 7.10 *(Source: www.spaceweather.com/archive.php)*

The Solar Flare of March 30, 2004

On the 30th of March, a solar flare was recorded independently by our own station using a computer spectrogram whilst connected remotely to the University of Florida Radio Observatory (UFRO) at 1759UT (0200 Local). The flare originated from sunspot group 570 (Images 7.7) and was again identified to be a Type III solar burst (Figure 7.11). No flare images were obtained due to a CCD bakeout of SOHO cameras. It was classified by GOES as a C1 flare measuring in at $1.0X10^{-6}$ Wm^{-2} (Figure 7.13). An observer located in Montana, USA provided us with the strip-chart verification of our recording (Figure 7.12). Again, no radio blackout was observed on both the spectrogram and strip-chart record (Figures 7.11 & 7.12).

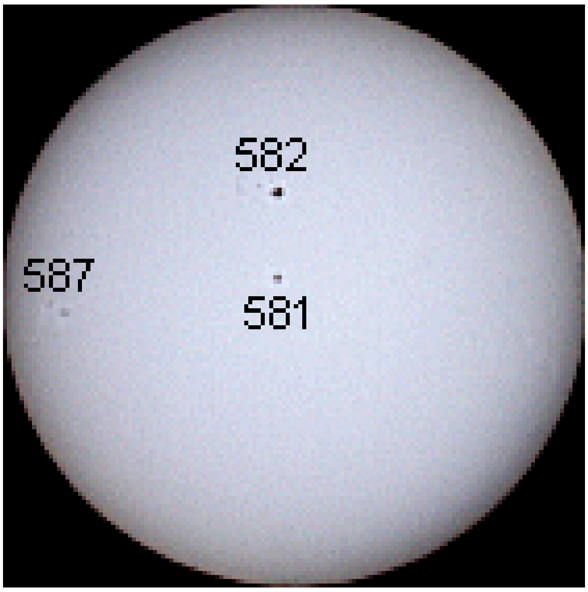

Image 7.7
(Source: www.spaceweather.com/archive.php)

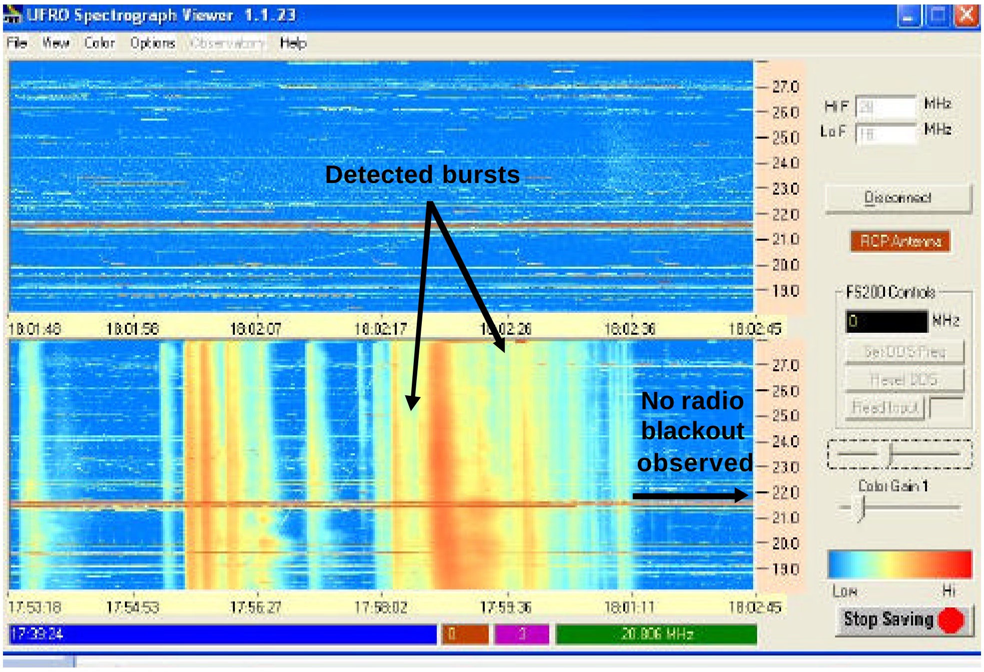

Figure 7.11

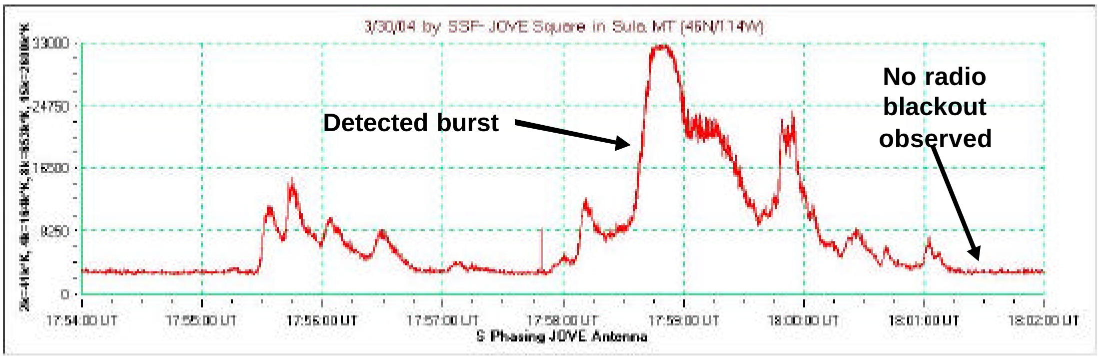

Figure 7.12

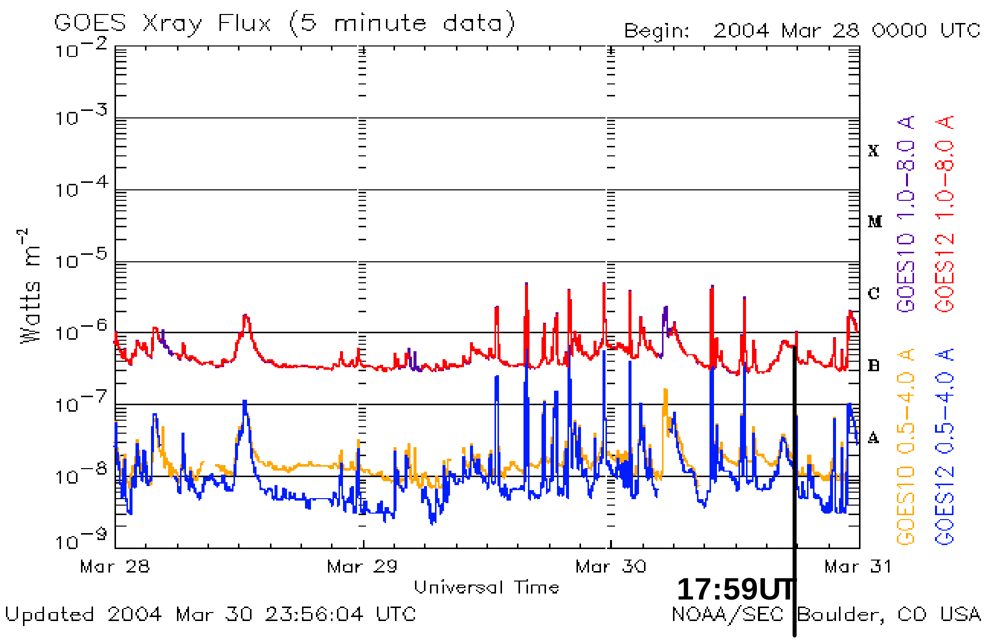

Figure 7.13 *(Source: www.spaceweather.com/archive.php)*

8. Analysis of Data Sources

The analysis of data sources was done using the strip-charts, spectrograms and GOES X-ray flux measurements for comparison of all four observations. Historical data was also used to further support our findings as well as a means of comparison.

By analysing and comparing historical data with the burst patterns of our strip-chart and spectrogram records, it was found that all 4 class flares had solar radio emissions in the decametric frequencies exhibiting Type III burst characteristics.

Our analysis has also shown that solar flares can cause radio blackouts. However, there is a trend to which radio blackout occurs. Of the 4 data sources collected, a radio blackout was observed only for the X and M class flares whilst the C and B class flares did not cause a radio blackout. The frequencies involved seem to be a function of the energy associated with the X-ray event, where the low frequency limit of the blackout is directly related to the magnitude of the X-ray flux.

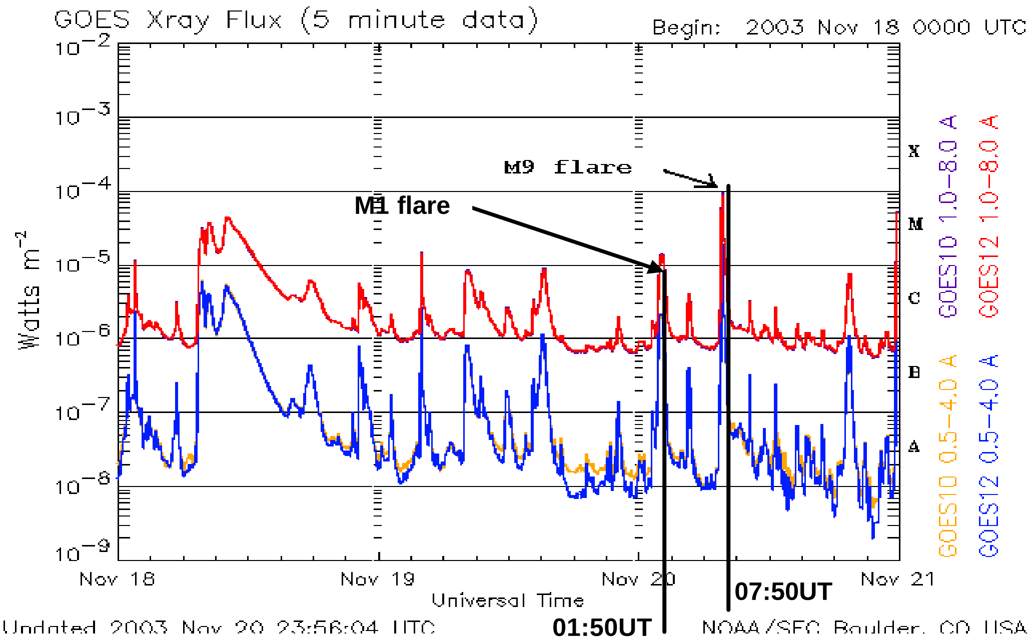

Figure 8.1 *(Source: www.spaceweather.com/archive.php)*

To explain this observation, we turned to the same IPS spectrogram recorded on the 20th of November 2003. On the same day as the M9 flare which our station detected, an earlier less powerful M1 flare with an X-ray flux density measuring 1.0X10^{-5} Wm^{-2} (Figure 8.1) was also recorded on the same spectrogram at 0150 UT. When the spectrograms of the two flares were compared, it was found that the radio blackout caused by the M9 flare suffered a greater "dip" along the Y-axis as compared to the M1 flare (Figures 8.2 & 8.3).

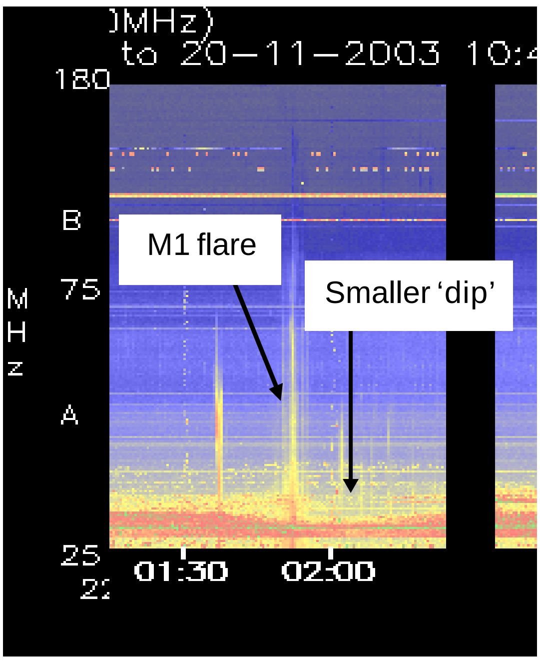

Figure 8.2 *(Source: www.ips.gov.au)*

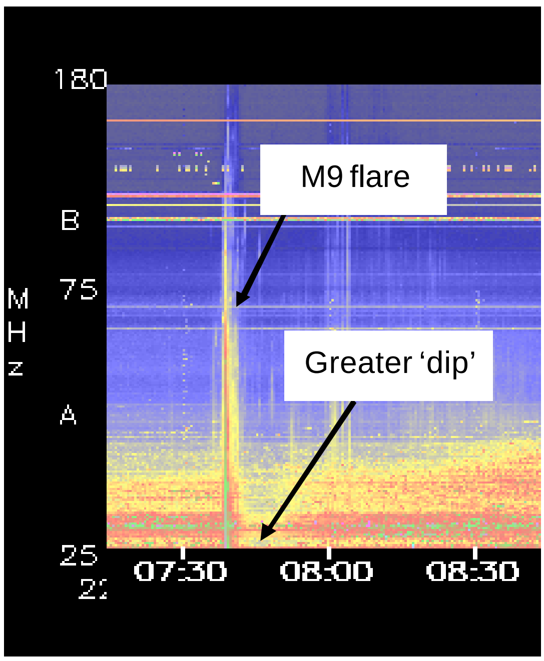

Figure 8.3 *(Source: www.ips.gov.au)*

When X-ray flux densities are low, only the upper band frequencies in the decametric range was found experiences a blackout whilst the lower frequencies do not (figure 8.2). This implies that as X-ray flux density rises, the number of frequencies experiencing a blackout increases downwards to encompass lower

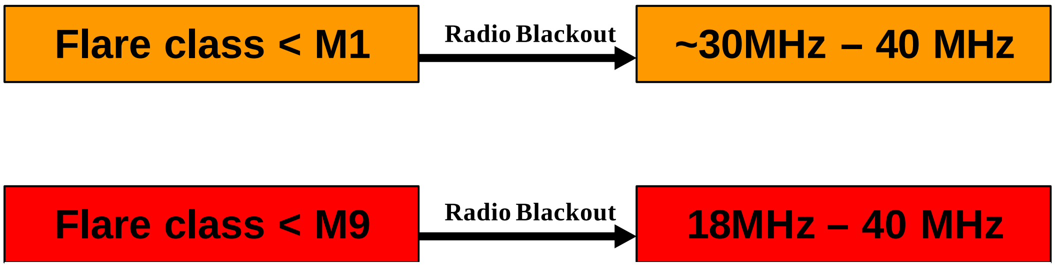

Chart 8.1

frequencies (Chart 8.1). As our strip-charts and spectrograms only record within the lower-mid decametric range of 19MHz to 27MHz, only radio blackouts due to powerful M & X class flares are recorded. This trend observed coincides with the NOAA Space Weather Scale for Radio Blackouts (Annex A) in which R5 (extreme) blackouts as a result of an X20 flare would cause signal losses in the entire decamtric range as compared to “limited frequencies” as a result of R1 (minor) blackouts . The probability of R1 blackouts due to less powerful flares is also found to be highest.

9. Conclusion

From our data analysis, we have made two conclusions:

A. Decametric frequencies are mostly affected by Type III solar bursts.

B. The band of frequencies experiencing radio blackouts in the decametric range increases from higher to lower frequencies as the degree of Ionisation in the ionosphere X-rays increases.

Research has shown that higher frequencies are refracted at higher altitudes (Wayne Tomasi, 1988) as illustrated in Figure 9.1. As to why radio blackouts at lower frequencies occur only if a solar flare greater than class M happens, we hypothesize that it is due to the extent of ionosphere ionisation. At low flux density levels, only upper portions of the ionosphere experiences X-ray ionisation and hence higher frequencies experience absorption. Therefore at high flux densities, X-rays are powerful enough to penetrate deeper into the atmosphere to cause ionisation at lower altitudes and the absorption of lower frequencies in the decametric range.

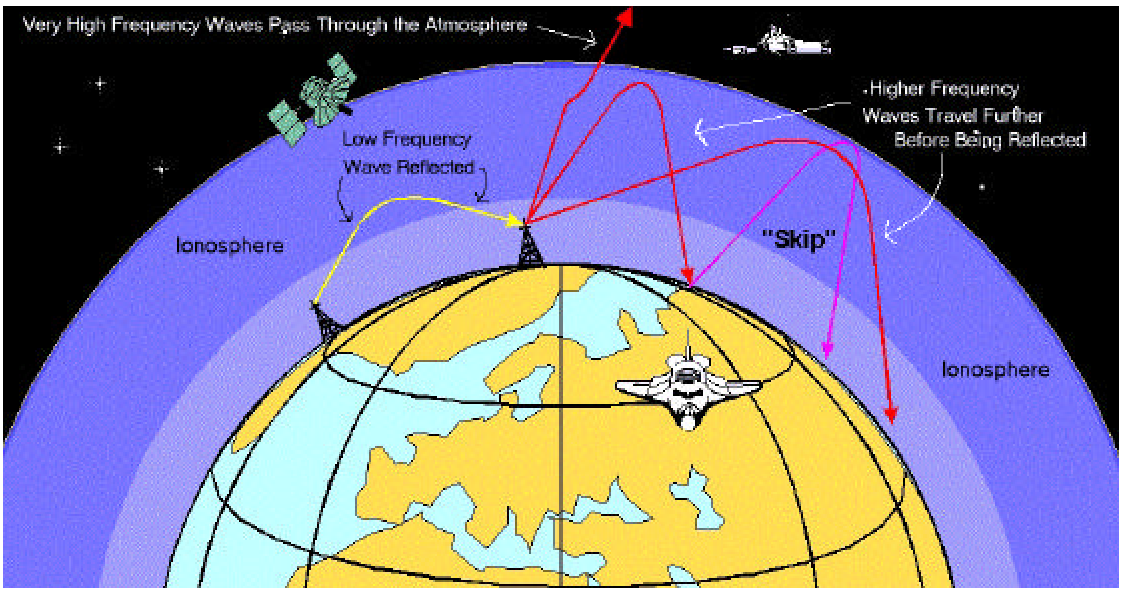

Figure 9.1 ***(Source:*** *www.voyager.co.nz/~elbate/propo.htm)*

10. Application

HF frequencies are commonly used in the telecommunication industry for long range communications due to its ability to bounce signals between the ionosphere and the Earth. Hence, it is widely used by the RSN (Republic of Singapore Navy), maritime operators and aviators to communicate and navigate. By investigating the effects of solar flares on HF propagation, we would now have a greater understanding of its detrimental effects on HF communications. Our report would thus be useful to these users as it would draw certain lessons to prepare them as well as to lay a foundation for future developments of counter-measures.

From our investigation, we have found that M1 flares occur the most frequent (Annex A) and causes blackouts between the frequencies of 30MHz – 40 MHz. Hence, we would like to advise that HF communication users operate at lower ends of the decametric range (15 MHz<) as it is less susceptible to most radio blackouts up to a M9 class solar flare. Due to the extensive usage of HF communication by the RSN, maritime operators and aviators, even a blackout lasting 5 minutes during any emergency could be a matter of life and death if users are unable to radio for help. For aviators relying on HF radio beacons to navigate via an ADF (Air Directional Finder) transponder, blackouts for brief intervals would affect aircraft navigations which are vital especially under poor weather and visibility conditions. Alternatively, VLF communications (50 KHz-150 KHz) could be used instead by propagating at lower altitudes (also known as tropospheric propagation) which are less affected by solar flares (Donald G. Fink, 1979).

It is difficult to prevent signal attenuation due to radio blackouts; however, we can still avoid it through pre-emptive action. We would like to propose that telecommunication and maritime authorities in Singapore use our study as a basis for further investigation into the effects of solar flares on HF propagation so as to devise an effective way of forecasting such events. One way of forecasting solar flares is by correlating the trends of flare occurrences with visible sunspots. Sunspots also serve as a rough guide to solar activity by noting their sizes as well as numbers. Studies have shown that increased sunspot numbers indicate rising solar activity while sunspot sizes merely reflect the magnitude of magnetic flux density in the sunspot region (Jay M. Pasachoff, 1979). These two indications could lead to a prediction of solar flare frequency as well as its magnitude. By forecasting radio-blackouts and broadcasting warnings in near real time over 3 hour intervals, it would allow HF users the advantage of preparing counter-measures for such events. This would firstly give time for operators to switch to lower frequencies if they are operating above 28MHz, and secondly, allow operators to increase transmitting power over a short period of time. By increasing the transmitting power, it gives HF signals a higher chance of surviving signal attenuations due to X-ray absorption in the ionosphere and would thus allow HF radio transmissions to continue despite a radio blackout occurrence.

We thus hope that through our study, users of HF telecommunication in the maritime and aviation industry would be able to gain a greater understanding of these effects and be able to prepare counter-measures to protect their systems and communications. We also hope to assist telecommunication authorities and companies to create a reliable forecasting system based on the trends which we have investigated.

11. Bibliography

Books

Forrest Barker (1987)
Communications Electronics: Systems, Circuits, and Devices
Chapter 6, pg 200 - 207
Prentice-Hall International

Peter Bubb (1984)
Understanding Radio Waves
Lutterworth Press

Donald G. Fink (1979)
Electronics Engineer's Handbook
McGraw-Hill Book Company

Richard S. Flagg (2000)
Listening to Jupiter
Chapter 5, pg 5-1 – 5-6
Radio-Sky Publishing

John D. Kraus (1986)
Radio Astronomy
Chapter 8, pg 8-52 – 8-56
Cygnus-Quasar Books

Jay M. Pasachoff (1979)
Astronomy: From the Earth to the Universe
Saunders Golden Sunburst

Wayne Tomasi (1988)
Fundamentals of Electronic Communications Systems
Chapter 10, pg 416 – 420
Prentice Hall

Internet URLs

National Oceanic and Atmospheric Administration
http://www.sec.noaa.gov

The Solar and Heliospheric Observatory
http://sohowww.nascom.nasa.gov/

The Australian Space Weather Service
http://www.ips.gov.au

Project Radio JOVE
http://radiojove.gsfc.nasa.gov

The National Association for Amateur Radio
http://www.arrl.org

SpaceWeather.com
http://www.spaceweather.com

Laboratory for Astronomy and Solar Physics
http://hesperia.gsfc.nasa.gov/sftheory/index.htm

Annex A

NOAA Space Weather Scale for Radio Blackouts

Category		Effect	Physical measure	Average Frequency (1 cycle = 11 years)
Scale	**Descriptor**	**Duration of event will influence severity of effects**		
Radio Blackouts			**GOES X-ray peak brightness by class and by flux***	**Number of events when flux level was met; (number of storm days)**
R 5	**Extreme**	**HF Radio:** Complete HF (high frequency**) radio blackout on the entire sunlit side of the Earth lasting for a number of hours. This results in no HF radio contact with mariners and en route aviators in this sector. **Navigation:** Low-frequency	X20 (2×10^{-3})	Less than 1 per cycle

		navigation signals used by maritime and general aviation systems experience outages on the sunlit side of the Earth for many hours, causing loss in positioning. Increased satellite navigation errors in positioning for several hours on the sunlit side of Earth, which may spread into the night side.		
R 4	**Severe**	**HF Radio:** : HF radio communication blackout on most of the sunlit side of Earth for one to two hours. HF radio contact lost during this time. **Navigation:** Outages of low-frequency navigation signals cause increased error in positioning for one to two hours. Minor disruptions of satellite navigation possible on the sunlit side of Earth.	X10 (10^{-3})	8 per cycle (8 days per cycle)
R 3	**Strong**	**HF Radio:** Wide area blackout of HF radio	X1 (10^{-4})	175 per cycle

		communication, loss of radio contact for about an hour on sunlit side of Earth. **Navigation:** Low-frequency navigation signals degraded for about an hour.		(140 days per cycle)
R 2	**Moderate**	**HF Radio:** Limited blackout of HF radio communication on sunlit side, loss of radio contact for tens of minutes. **Navigation:** Degradation of low-frequency navigation signals for tens of minutes.	M5 (5×10^{-5})	350 per cycle (300 days per cycle)
R 1	**Minor**	**HF Radio:** Weak or minor degradation of HF radio communication on sunlit side, occasional loss of radio contact. **Navigation:** Low-frequency navigation signals degraded for brief intervals.	M1 (10^{-5})	2000 per cycle (950 days per cycle)

Table Credit: http://www.sec.noaa.gov/NOAAscales/#RadioBlackouts